

An introduction to Hybrid High-Order methods with application to the incompressible Navier–Stokes equations











































Daniele A. Di Pietro

Institut Montpelliérain Alexander Grothendieck, University of Montpellier

Udine, 30 October 2018



HHO: The inner circle

- Joubine Aghili (Université de Nice  )
- Sébastien Boyaval (École des Ponts ParisTech  )
- Daniele Boffi (Università di Pavia  )
- Francesco Bonaldi (Politecnico di Milano  )
- Lorenzo Botti (Università di Bergamo  )
- Michele Botti (Université de Montpellier  )
- Florent Chave (Université de Montpellier   and Politecnico di Milano  )
- Bernardo Cockburn (University of Minnesota )
- Jérôme Droniou (Monash University )
- Alexandre Ern (École des Ponts ParisTech  )
- Luca Formaggia (Politecnico di Milano  )
- Giuseppe Geymonat (École Polytechnique  )
- Françoise Krasucki (Université de Montpellier  )
- Stella Krell (Université de Nice  )
- Simon Lemaire (INRIA  )
- Alexander Linke (Weierstraß Institute Berlin )
- Gianmarco Manzini (Los Alamos National Laboratories )
- Fabien Marche (Université de Montpellier  )
- Franck Pigeonneau (Saint-Gobain Recherche  )
- Berardo Ruffini (Université de Montpellier  )
- Friedhelm Schieweck (Otto-von-Güricke Universität )
- Pierre Sochala (BRGM  )
- Ruben Specogna (Università di Udine  )
- ...



Features

- Capability of handling **general polyhedral meshes**
- Construction valid for **arbitrary space dimensions**
- Arbitrary **approximation order** (including $k = 0$)
- **Robustness** with respect to the variations of the physical coefficients
- Reduced **computational cost** after static condensation

- 1 Basics of HHO methods
- 2 Application to the incompressible Navier–Stokes problem

- 1 Basics of HHO methods
- 2 Application to the incompressible Navier–Stokes problem

- **Discrete unknowns** at elements and faces
- **Local reconstructions** inspired from local projectors
- No explicit expression for the basis functions
- **High-order stabilisation** inside each element
- **Fully discrete formulation** [DP and Droniou, 2018]

Polyhedral meshes

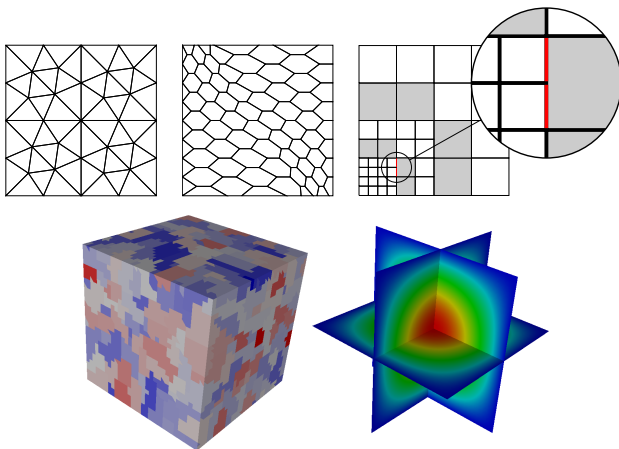


Figure: Supported meshes in 2d and 3d, and HHO solution on the agglomerated 3d mesh. For the notions of polytopal mesh and regular polytopal mesh sequence see [DP and Tittarelli, 2018]

Model problem

- Let $\Omega \subset \mathbb{R}^d$, $d \geq 1$, denote a bounded, connected polyhedral domain
- For $f \in L^2(\Omega)$, we consider the **Poisson problem**

$$\begin{aligned} -\Delta u &= f && \text{in } \Omega \\ u &= 0 && \text{on } \partial\Omega \end{aligned}$$

- In weak form: Find $u \in H_0^1(\Omega)$ s.t.

$$a(u, v) := (\nabla u, \nabla v) = (f, v) \quad \forall v \in H_0^1(\Omega)$$

Projectors on local polynomial spaces

- At the core of HHO are **projectors on local polynomial spaces**
- With $X = T$ or $X = F$, the **L^2 -projector** $\pi_X^{0,l} : L^1(X) \rightarrow \mathbb{P}^l(X)$ is s.t.

$$(\pi_X^{0,l} v - v, w)_X = 0 \text{ for all } w \in \mathbb{P}^l(X)$$

- The **elliptic projector** $\pi_T^{1,l} : W^{1,1}(T) \rightarrow \mathbb{P}^l(T)$ is s.t.

$$(\nabla(\pi_T^{1,l} v - v), \nabla w)_T = 0 \text{ for all } w \in \mathbb{P}^l(T) \text{ and } \int_T (\pi_T^{1,l} v - v) = 0$$

- Both $\pi_T^{0,l}$ and $\pi_T^{1,l}$ have **optimal approximation properties in $\mathbb{P}^l(T)$**
- See [DP and Droniou, 2017a, DP and Droniou, 2017b]

Computing $\pi_T^{1,k+1}$ from L^2 -projections of degree k

- Recall the following IBP valid for all $v \in H^1(T)$ and all $w \in C^\infty(\bar{T})$:

$$(\nabla v, \nabla w)_T = -(v, \Delta w)_T + \sum_{F \in \mathcal{F}_T} (v, \nabla w \cdot \mathbf{n}_{TF})_F$$

- Specializing it to $w \in \mathbb{P}^{k+1}(T)$, we can write

$$(\nabla \pi_T^{1,k+1} v, \nabla w)_T = -(\pi_T^{0,k} v, \Delta w)_T + \sum_{F \in \mathcal{F}_T} (\pi_F^{0,k} v|_F, \nabla w \cdot \mathbf{n}_{TF})_F$$

- Moreover, it can be easily seen that

$$\int_T (\pi_T^{1,k+1} v - v) = \int_T (\pi_T^{1,k+1} v - \pi_T^{0,k} v) = 0$$

- Hence, $\pi_T^{1,k+1} v$ can be computed from $\pi_T^{0,k} v$ and $(\pi_F^{0,k} v|_F)_{F \in \mathcal{F}_T}$!**

Discrete unknowns

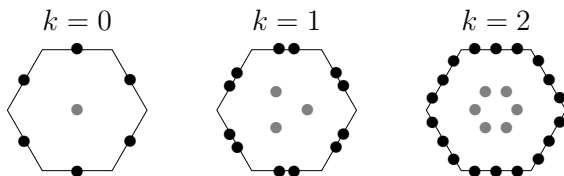


Figure: \underline{U}_T^k for $k \in \{0, 1, 2\}$

- Let a polynomial degree $k \geq 0$ be fixed
- For all $T \in \mathcal{T}_h$, we define the **local space of discrete unknowns**

$$\underline{U}_T^k := \{ \underline{v}_T = (v_T, (v_F)_{F \in \mathcal{F}_T}) : v_T \in \mathbb{P}^k(T) \text{ and } v_F \in \mathbb{P}^k(F) \quad \forall F \in \mathcal{F}_T \}$$

- The **local interpolator** $\underline{I}_T^k : H^1(T) \rightarrow \underline{U}_T^k$ is s.t., for all $v \in H^1(T)$,

$$\underline{I}_T^k v := (\pi_T^{0,k} v, (\pi_F^{0,k} v|_F)_{F \in \mathcal{F}_T})$$

Local potential reconstruction

- Let $T \in \mathcal{T}_h$. We define the local **potential reconstruction** operator

$$r_T^{k+1} : \underline{U}_T^k \rightarrow \mathbb{P}^{k+1}(T)$$

s.t. for all $\underline{v}_T \in \underline{U}_T^k$, $\int_T (r_T^{k+1} \underline{v}_T - v_T) = 0$ and

$$\boxed{(\nabla r_T^{k+1} \underline{v}_T, \nabla w)_T = -(v_T, \Delta w)_T + \sum_{F \in \mathcal{F}_T} (v_F, \nabla w \cdot \mathbf{n}_{TF})_F \quad \forall w \in \mathbb{P}^{k+1}(T)}$$

- By construction, we have

$$\boxed{r_T^{k+1} \circ \underline{I}_T^k = \pi_T^{1,k+1}}$$

- $r_T^{k+1} \circ \underline{I}_T^k$ has therefore **optimal approximation properties** in $\mathbb{P}^{k+1}(T)$

- We would be tempted to approximate

$$a_T(u, v) \approx (\nabla r_T^{k+1} \underline{u}_T, \nabla r_T^{k+1} \underline{v}_T)_T$$

- This choice, however, is **not stable** in general. We consider instead

$$a_T(\underline{u}_T, \underline{v}_T) := (\nabla r_T^{k+1} \underline{u}_T, \nabla r_T^{k+1} \underline{v}_T)_T + s_T(\underline{u}_T, \underline{v}_T)$$

- The role of s_T is to ensure **$\|\cdot\|_{1,T}$ -coercivity** with

$$\|\underline{v}_T\|_{1,T}^2 := \|\nabla v_T\|_T^2 + \sum_{F \in \mathcal{F}_T} \frac{1}{h_F} \|v_F - v_T\|_F^2 \quad \forall \underline{v}_T \in \underline{U}_T^k$$

Assumption (Stabilization bilinear form)

The bilinear form $s_T : \underline{U}_T^k \times \underline{U}_T^k \rightarrow \mathbb{R}$ satisfies the following properties:

- **Symmetry and positivity.** s_T is symmetric and positive semidefinite.
- **Stability.** It holds, with hidden constant independent of h and T ,

$$a_T(\underline{v}_T, \underline{v}_T)^{\frac{1}{2}} \simeq \|\underline{v}_T\|_{1,T} \quad \forall \underline{v}_T \in \underline{U}_T^k.$$

- **Polynomial consistency.** For all $w \in \mathbb{P}^{k+1}(T)$ and all $\underline{v}_T \in \underline{U}_T^k$,

$$s_T(\underline{I}_T^k w, \underline{v}_T) = 0.$$

- The following stable choice **violates polynomial consistency**:

$$s_T^{\text{hdg}}(\underline{u}_T, \underline{v}_T) := \sum_{F \in \tilde{\mathcal{F}}_T} h_F^{-1} (u_F - u_T, v_F - v_T)_F$$

- To circumvent this problem, we penalize the **high-order differences**

$$(\delta_T^k \underline{v}_T, (\delta_{TF}^k \underline{v}_T)_{F \in \mathcal{F}_T}) := \underline{I}_T^k r_T^{k+1} \underline{v}_T - \underline{v}_T$$

- The classical HHO stabilization bilinear form reads

$$s_T(\underline{u}_T, \underline{v}_T) := \sum_{F \in \tilde{\mathcal{F}}_T} h_F^{-1} ((\delta_T^k - \delta_{TF}^k) \underline{u}_T, (\delta_T^k - \delta_{TF}^k) \underline{v}_T)_F$$

Discrete problem

- Define the **global space** with single-valued interface unknowns

$$\underline{U}_h^k := \left\{ \underline{v}_h = ((v_T)_{T \in \mathcal{T}_h}, (v_F)_{F \in \mathcal{F}_h}) : \right. \\ \left. v_T \in \mathbb{P}^k(T) \quad \forall T \in \mathcal{T}_h \text{ and } v_F \in \mathbb{P}^k(F) \quad \forall F \in \mathcal{F}_h \right\}$$

and its subspace with **strongly enforced boundary conditions**

$$\underline{U}_{h,0}^k := \{ \underline{v}_h \in \underline{U}_h^k : v_F = 0 \quad \forall F \in \mathcal{F}_h^b \}$$

- The discrete problem reads: Find $\underline{u}_h \in \underline{U}_{h,0}^k$ s.t.

$$\mathbf{a}_h(\underline{u}_h, \underline{v}_h) := \sum_{T \in \mathcal{T}_h} \mathbf{a}_T(\underline{u}_T, \underline{v}_T) = \sum_{T \in \mathcal{T}_h} (f, v_T)_T \quad \forall \underline{v}_h \in \underline{U}_{h,0}^k$$

- Well-posedness** follows from coercivity and discrete Poincaré

Convergence

Theorem (Energy-norm error estimate)

Assume $u \in H_0^1(\Omega) \cap H^{k+2}(\mathcal{T}_h)$. The following energy error estimate holds:

$$\|\nabla_h(r_h^{k+1}\underline{u}_h - u)\| + |\underline{u}_h|_{s,h} \lesssim h^{k+1}|u|_{H^{k+2}(\mathcal{T}_h)},$$

with $(r_h^{k+1}\underline{u}_h)|_T := r_T^{k+1}\underline{u}_T$ for all $T \in \mathcal{T}_h$ and $|\underline{u}_h|_{s,h}^2 := \sum_{T \in \mathcal{T}_h} s_T(\underline{u}_T, \underline{u}_T)$.

Theorem (Superclose L^2 -norm error estimate)

Further assuming *elliptic regularity* and $f \in H^1(\mathcal{T}_h)$ if $k = 0$,

$$\|r_h^{k+1}\underline{u}_h - u\| \lesssim h^{k+2}\mathcal{N}_k,$$

with $\mathcal{N}_0 := \|f\|_{H^1(\mathcal{T}_h)}$ and $\mathcal{N}_k := |u|_{H^{k+2}(\mathcal{T}_h)}$ for $k \geq 1$.

Static condensation I

- Fix a basis for $\underline{U}_{h,0}^k$ with functions supported by only one T or F
- Partition the discrete unknowns into **element-** and **interface-based**:

$$U_h = \begin{bmatrix} U_{\mathcal{T}_h} \\ U_{\mathcal{F}_h^i} \end{bmatrix}$$

- U_h solves the following linear system:

$$\begin{bmatrix} A_{\mathcal{T}_h \mathcal{T}_h} & A_{\mathcal{T}_h \mathcal{F}_h^i} \\ A_{\mathcal{F}_h^i \mathcal{T}_h} & A_{\mathcal{F}_h^i \mathcal{F}_h^i} \end{bmatrix} \begin{bmatrix} U_{\mathcal{T}_h} \\ U_{\mathcal{F}_h^i} \end{bmatrix} = \begin{bmatrix} F_{\mathcal{T}_h} \\ 0 \end{bmatrix}$$

- $A_{\mathcal{T}_h \mathcal{T}_h}$ is **block-diagonal and SPD, hence inexpensive to invert**

This remark suggests a **two-step solution strategy**:

- Element unknowns are eliminated solving the **local balances**

$$U_{\mathcal{T}_h} = A_{\mathcal{T}_h \mathcal{T}_h}^{-1} \left(F_{\mathcal{T}_h} - A_{\mathcal{T}_h \mathcal{F}_h^i} U_{\mathcal{F}_h^i} \right)$$

- Face unknowns are obtained solving the **global transmission problem**

$$A_h^{\text{SC}} U_{\mathcal{F}_h^i} = -A_{\mathcal{T}_h \mathcal{F}_h}^T A_{\mathcal{T}_h \mathcal{T}_h}^{-1} F_{\mathcal{T}_h}$$

with global system matrix

$$A_h^{\text{SC}} := A_{\mathcal{F}_h \mathcal{F}_h} - A_{\mathcal{T}_h \mathcal{F}_h}^T A_{\mathcal{T}_h \mathcal{T}_h}^{-1} A_{\mathcal{T}_h \mathcal{F}_h}$$

- A_h^{SC} is **SPD** and its stencil involves neighbours through faces

Numerical examples

2d test case, smooth solution, uniform refinement

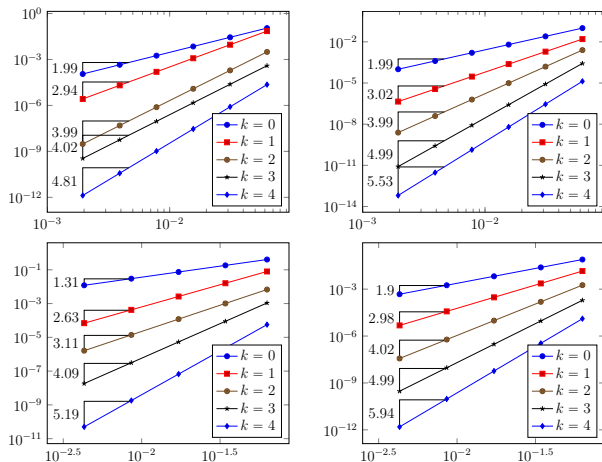


Figure: 2d test case, trigonometric solution. Energy (left) and L^2 -norm (right) of the error vs. h for uniformly refined **triangular** (top) and **hexagonal** (bottom) mesh families

Numerical examples I

3d industrial test case, adaptive refinement, cost assessment

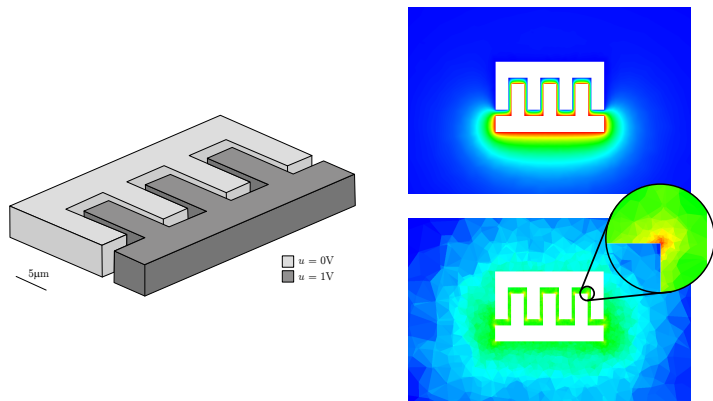
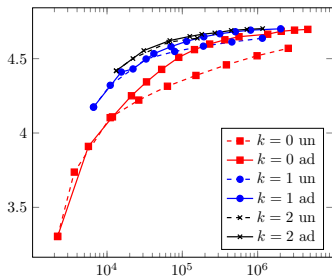


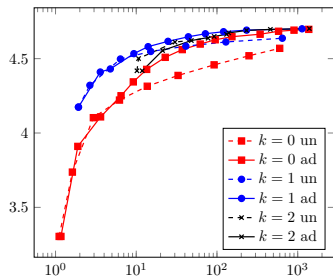
Figure: Geometry (left), numerical solution (right, top) and final adaptive mesh (right, bottom) for the comb-drive actuator test case [DP and Specogna, 2016]

Numerical examples II

3d industrial test case, adaptive refinement, cost assessment



(a) Capacitance vs. $N_{\text{dof},h}$

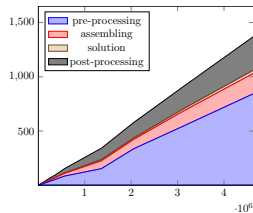


(b) Capacitance vs. computing time

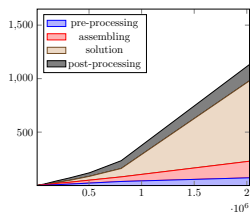
Figure: Results for the comb drive benchmark.

Numerical examples III

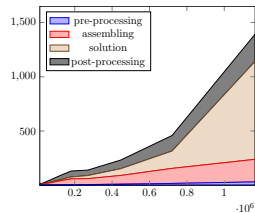
3d industrial test case, adaptive refinement, cost assessment



(a) $k = 0$



(b) $k = 1$



(c) $k = 2$

Figure: Computing wall time (s) vs. number of DOFs for the comb drive benchmark, AGMG solver.

Numerical examples I

3d test case, singular solution, adaptive coarsening

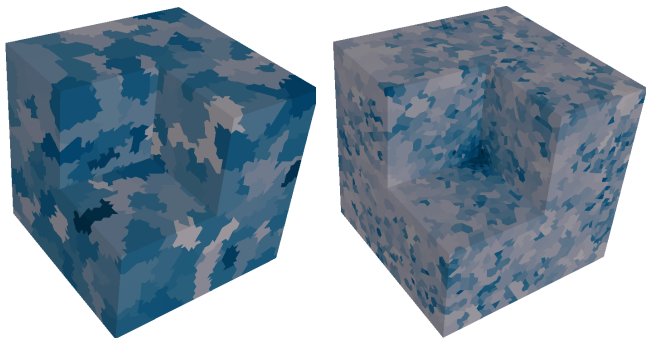
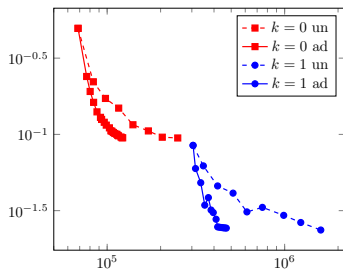


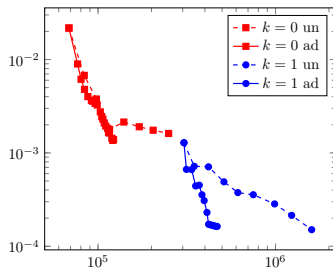
Figure: Fichera corner benchmark, adaptive mesh coarsening [DP and Specogna, 2016]

Numerical examples II

3d test case, singular solution, adaptive coarsening



(a) Energy-error vs. N_{dofs}



(b) L^2 -error vs. N_{dof}

Figure: Error vs. number of DOFs for the Fichera corner benchmark, adaptively coarsened meshes

- 1 Basics of HHO methods
- 2 Application to the incompressible Navier–Stokes problem

- Capability of handling **general polyhedral meshes**
- Construction valid for both $d = 2$ and $d = 3$
- Arbitrary **approximation order** (including $k = 0$)
- **Inf-sup stability** on general meshes
- **Robust handling** of dominant advection
- **Local conservation** of momentum and mass
- Reduced **computational cost** after static condensation

$$N_{\text{dof},h} = d \operatorname{card}(\mathcal{F}_h^i) \binom{k-1+d}{d-1} + \operatorname{card}(\mathcal{T}_h)$$

HHO for incompressible flows

- MHO for Stokes [Aghili, Boyaval, DP, 2015]
- Pressure-robust HHO for Stokes [DP, Ern, Linke, Schieweck, 2016]
- Péclet-robust HHO for Oseen [Aghili and DP, 2018]
- Darcy-robust HHO for Brinkman [Botti, DP, Droniou, 2018]
- Skew-symmetric HHO for Navier–Stokes [DP and Krell, 2018]
- Temam's device for HHO [Botti, DP, Droniou, 2018]

The incompressible Navier–Stokes equations I

- Let $d \in \{2, 3\}$, $\nu \in \mathbb{R}_+^*$, $\mathbf{f} \in L^2(\Omega)^d$, $\mathbf{U} := H_0^1(\Omega)^d$, and $P := L_0^2(\Omega)$
- The INS problem reads: Find $(\mathbf{u}, p) \in \mathbf{U} \times P$ s.t.

$$\begin{aligned} \nu a(\mathbf{u}, \mathbf{v}) + t(\mathbf{u}, \mathbf{u}, \mathbf{v}) + b(\mathbf{v}, p) &= \int_{\Omega} \mathbf{f} \cdot \mathbf{v} & \forall \mathbf{v} \in \mathbf{U}, \\ -b(\mathbf{u}, q) &= 0 & \forall q \in L^2(\Omega), \end{aligned}$$

with **viscous** and **pressure-velocity coupling bilinear forms**

$$a(\mathbf{w}, \mathbf{v}) := \int_{\Omega} \nabla \mathbf{w} : \nabla \mathbf{v}, \quad b(\mathbf{v}, q) := - \int_{\Omega} q \nabla \cdot \mathbf{v}$$

and **convective trilinear form**

$$t(\mathbf{w}, \mathbf{v}, \mathbf{z}) := \int_{\Omega} (\mathbf{w} \cdot \nabla) \mathbf{v} \cdot \mathbf{z} = \sum_{i=1}^d \sum_{j=1}^d \int_{\Omega} w_j (\partial_j v_i) z_i$$

Discrete spaces I

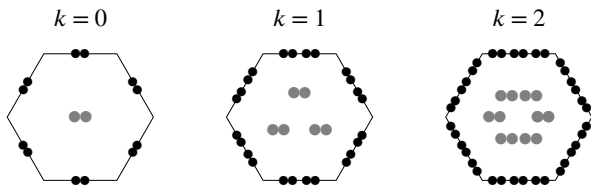


Figure: Local velocity space \underline{U}_T^k for $k \in \{0, 1, 2\}$

- For $k \geq 0$, we define the **global space of discrete velocity unknowns**

$$\underline{U}_h^k := \left\{ \underline{\mathbf{v}}_h = ((\mathbf{v}_T)_{T \in \mathcal{T}_h}, (\mathbf{v}_F)_{F \in \mathcal{F}_h}) : \right. \\ \left. \mathbf{v}_T \in \mathbb{P}^k(T)^d \quad \forall T \in \mathcal{T}_h \text{ and } \mathbf{v}_F \in \mathbb{P}^k(F)^d \quad \forall F \in \mathcal{F}_h \right\}$$

- The restrictions to $T \in \mathcal{T}_h$ are \underline{U}_T^k and $\underline{\mathbf{v}}_T = (\mathbf{v}_T, (\mathbf{v}_F)_{F \in \mathcal{F}_T})$

Discrete spaces II

- The **global interpolator** $\underline{I}_h^k : H^1(\Omega)^d \rightarrow \underline{U}_h^k$ is s.t., $\forall \mathbf{v} \in H^1(\Omega)^d$,

$$\underline{I}_h^k \mathbf{v} := \left((\boldsymbol{\pi}_T^{0,k} \mathbf{v}|_T)_{T \in \mathcal{T}_h}, (\boldsymbol{\pi}_F^{0,k} \mathbf{v}|_F)_{F \in \mathcal{F}_h} \right)$$

- The **velocity space** strongly accounting for boundary conditions is

$$\underline{U}_{h,0}^k := \{ \underline{\mathbf{v}}_h \in \underline{U}_h^k : \mathbf{v}_F = \mathbf{0} \quad \forall F \in \mathcal{F}_h^b \}$$

equipped with the H_0^1 -like norm $\|\cdot\|_{1,h}$

- The **discrete pressure space** is defined setting

$$P_h^k := \left\{ q_h \in \mathbb{P}^k(\mathcal{T}_h) : \int_{\Omega} q_h = 0 \right\} \subset P$$

Gradient, velocity, and divergence reconstructions I

- We define local reconstructions mimicking integration by parts on T
- For $\ell \geq 0$, the **gradient reconstruction** $\mathbf{G}_T^\ell : \underline{U}_T^k \rightarrow \mathbb{P}^\ell(T)^{d \times d}$ is s.t.

$$\int_T \mathbf{G}_T^\ell \underline{v}_T : \boldsymbol{\tau} = - \int_T \mathbf{v}_T \cdot (\nabla \cdot \boldsymbol{\tau}) + \sum_{F \in \mathcal{F}_T} \int_F \mathbf{v}_F \cdot (\boldsymbol{\tau} \mathbf{n}_{TF}) \quad \forall \boldsymbol{\tau} \in \mathbb{P}^\ell(T)^{d \times d}$$

- The **velocity reconstruction**

$$\mathbf{r}_T^{k+1} : \underline{U}_T^k \rightarrow \mathbb{P}^{k+1}(T)^d$$

is s.t. $\int_T (\mathbf{r}_T^{k+1} \underline{v}_T - \mathbf{v}_T) = \mathbf{0}$ and

$$\int_T (\nabla \mathbf{r}_T^{k+1} \underline{v}_T - \mathbf{G}_T^k \underline{v}_T) : \nabla \mathbf{w} = 0 \quad \forall \mathbf{w} \in \mathbb{P}^{k+1}(T)^d$$

- The **divergence reconstruction** $D_T^\ell : \underline{U}_T^k \rightarrow \mathbb{P}^\ell(T)$ is s.t.

$$D_T^\ell \underline{v}_T := \text{tr}(\mathbf{G}_T^\ell \underline{v}_T)$$

- The **viscous term** is discretized by means of the bilinear form a_h s.t.

$$a_h(\underline{\mathbf{u}}_h, \underline{\mathbf{v}}_h) := \sum_{T \in \mathcal{T}_h} a_T(\underline{\mathbf{u}}_T, \underline{\mathbf{v}}_T)$$

with local contribution

$$a_T(\underline{\mathbf{w}}_T, \underline{\mathbf{v}}_T) := (\nabla \mathbf{r}_T^{k+1} \underline{\mathbf{w}}_T, \nabla \mathbf{r}_T^{k+1} \underline{\mathbf{v}}_T)_T + s_T(\underline{\mathbf{w}}_T, \underline{\mathbf{v}}_T)$$

- As in the scalar case, several possible choices for s_h ensure that

$$a_h(\underline{\mathbf{v}}_h, \underline{\mathbf{v}}_h) \simeq \|\underline{\mathbf{v}}_h\|_{1,h}^2 \quad \forall \underline{\mathbf{v}}_h \in \underline{\mathbf{U}}_h^k$$

with real number C_a independent of h and of the problem data

- **Variable viscosity** can be treated following [DP and Ern, 2015]

Pressure-velocity coupling

- The **pressure-velocity coupling** is realized by means of

$$b_h(\underline{\mathbf{v}}_h, q_h) := - \sum_{T \in \mathcal{T}_h} \int_T D_T^k \underline{\mathbf{v}}_T q_T$$

- A crucial point is that b_h satisfies the following uniform **inf-sup condition**: There is $\beta > 0$ independent of h s.t.

$$\forall q_h \in P_h^k, \quad \beta \|q_h\|_{L^2(\Omega)} \leq \sup_{\underline{\mathbf{v}}_h \in \underline{\mathbf{U}}_{h,0}^k, \|\underline{\mathbf{v}}_h\|_{1,h}=1} b_h(\underline{\mathbf{v}}_h, q_h)$$

- This stability result is valid on **general meshes** and for any $k \geq 0$

A key remark I

- We have the following IBP formula: For all $\mathbf{w}, \mathbf{v}, \mathbf{z} \in H^1(\Omega)^d$,

$$\int_{\Omega} (\mathbf{w} \cdot \nabla) \mathbf{v} \cdot \mathbf{z} + \int_{\Omega} (\mathbf{w} \cdot \nabla) \mathbf{z} \cdot \mathbf{v} + \int_{\Omega} (\nabla \cdot \mathbf{w})(\mathbf{v} \cdot \mathbf{z}) = \int_{\partial\Omega} (\mathbf{w} \cdot \mathbf{n})(\mathbf{v} \cdot \mathbf{z})$$

- Using this formula with $\mathbf{w} = \mathbf{v} = \mathbf{z} = \mathbf{u}$, we get

$$t(\mathbf{u}, \mathbf{u}, \mathbf{u}) = \int_{\Omega} (\mathbf{u} \cdot \nabla) \mathbf{u} \cdot \mathbf{u} = -\frac{1}{2} \int_{\Omega} (\nabla \cdot \mathbf{u})(\mathbf{u} \cdot \mathbf{u}) + \frac{1}{2} \int_{\partial\Omega} (\mathbf{u} \cdot \mathbf{n})(\mathbf{u} \cdot \mathbf{u}) = 0,$$

where we have used the **mass equation** and the **boundary condition**

- This shows that the convective term is **non-dissipative**
- **This is a key property to mimic at the discrete level**

A key remark II

- The discrete velocity may not be divergence-free (and zero on $\partial\Omega$)
- We can use as a starting point modified versions of t :

$$t^{ss}(\mathbf{w}, \mathbf{v}, \mathbf{z}) := \frac{1}{2} \int_{\Omega} (\mathbf{w} \cdot \nabla) \mathbf{v} \cdot \mathbf{z} - \frac{1}{2} \int_{\Omega} (\mathbf{w} \cdot \nabla) \mathbf{z} \cdot \mathbf{v}$$

or, following [Temam, 1979],

$$t^{tm}(\mathbf{w}, \mathbf{v}, \mathbf{z}) := \int_{\Omega} (\mathbf{w} \cdot \nabla) \mathbf{v} \cdot \mathbf{z} + \frac{1}{2} \int_{\Omega} (\nabla \cdot \mathbf{w})(\mathbf{v} \cdot \mathbf{z}) - \frac{1}{2} \int_{\partial\Omega} (\mathbf{w} \cdot \mathbf{n})(\mathbf{v} \cdot \mathbf{z})$$

- For $\star \in \{tm, ss\}$ and all $\mathbf{w}, \mathbf{v} \in H^1(\Omega)^d$,

$$t^{\star}(\mathbf{w}, \mathbf{v}, \mathbf{v}) = 0$$

- Hence t^{\star} is non-dissipative even if $\nabla \cdot \mathbf{w} \neq 0$ and $\mathbf{v}|_{\partial\Omega} \neq 0$

Directional derivative reconstruction

- Let $\underline{w}_T \in \underline{U}_T^k$ represent a **velocity field on T**
- We let the **directional derivative reconstruction**

$$G_T^k(\underline{w}_T; \cdot) : \underline{U}_T^k \rightarrow \mathbb{P}^k(T)^d$$

is s.t., for all $\mathbf{z} \in \mathbb{P}^k(T)^d$,

$$\int_T G_T^k(\underline{w}_T; \underline{v}_T) \cdot \mathbf{z} = \int_T (\mathbf{w}_T \cdot \nabla) \mathbf{v}_T \cdot \mathbf{z} + \sum_{F \in \mathcal{F}_T} \int_F (\mathbf{w}_F \cdot \mathbf{n}_{TF}) (\mathbf{v}_F - \mathbf{v}_T) \cdot \mathbf{z}$$

- $G_T^k(\underline{w}_T; \underline{v}_T)$ and $\mathbf{G}_T^{2k} \underline{v}_T$ are linked: For all $\mathbf{z} \in \mathbb{P}^k(T)^d$,

$$\int_T G_T^k(\underline{w}_T; \underline{v}_T) \cdot \mathbf{z} = \int_T (\mathbf{w}_T \cdot \mathbf{G}_T^{2k}) \underline{v}_T \cdot \mathbf{z} + \sum_{F \in \mathcal{F}_T} \int_F (\mathbf{w}_F - \mathbf{w}_T) \cdot \mathbf{n}_{TF} (\mathbf{v}_F - \mathbf{v}_T) \cdot \mathbf{z}$$

Discrete global integration by parts formula

We mimick at the discrete level the formula:

$$\int_{\Omega} (\mathbf{w} \cdot \nabla) \mathbf{v} \cdot \mathbf{z} + \int_{\Omega} (\mathbf{w} \cdot \nabla) \mathbf{z} \cdot \mathbf{v} + \int_{\Omega} (\nabla \cdot \mathbf{w})(\mathbf{v} \cdot \mathbf{z}) = \int_{\partial\Omega} (\mathbf{w} \cdot \mathbf{n})(\mathbf{v} \cdot \mathbf{z})$$

Proposition (Discrete integration by parts formula)

It holds, for all $\underline{\mathbf{w}}_h, \underline{\mathbf{v}}_h, \underline{\mathbf{z}}_h \in \underline{U}_h^k$,

$$\begin{aligned} & \sum_{T \in \mathcal{T}_h} \int_T \left(G_T^k(\underline{\mathbf{w}}_T; \underline{\mathbf{v}}_T) \cdot \mathbf{z}_T + \mathbf{v}_T \cdot G_T^k(\underline{\mathbf{w}}_T; \underline{\mathbf{z}}_T) + D_T^{2k} \underline{\mathbf{w}}_T(\mathbf{v}_T \cdot \mathbf{z}_T) \right) \\ &= \sum_{F \in \mathcal{F}_h^b} \int_F (\mathbf{w}_F \cdot \mathbf{n}_F) \mathbf{v}_F \cdot \mathbf{z}_F - \sum_{T \in \mathcal{T}_h} \sum_{F \in \mathcal{F}_T} \int_F (\mathbf{w}_F \cdot \mathbf{n}_{TF}) (\mathbf{v}_F - \mathbf{v}_T) \cdot (\mathbf{z}_F - \mathbf{z}_T). \end{aligned}$$

The term in red reflects the *non-conformity* of the method.

Convective term I

$$t^{\text{tm}}(\mathbf{w}, \mathbf{v}, \mathbf{z}) := \int_{\Omega} (\mathbf{w} \cdot \nabla) \mathbf{v} \cdot \mathbf{z} + \frac{1}{2} \int_{\Omega} (\nabla \cdot \mathbf{w})(\mathbf{v} \cdot \mathbf{z}) \quad \forall \mathbf{w}, \mathbf{v}, \mathbf{z} \in \mathbf{U}$$

- Inspired by t^{tm} , we set

$$t_h(\underline{\mathbf{w}}_h, \underline{\mathbf{v}}_h, \underline{\mathbf{z}}_h) := \sum_{T \in \mathcal{T}_h} t_T(\underline{\mathbf{w}}_T, \underline{\mathbf{v}}_T, \underline{\mathbf{z}}_T)$$

where, for all $T \in \mathcal{T}_h$,

$$t_T(\underline{\mathbf{w}}_T, \underline{\mathbf{v}}_T, \underline{\mathbf{z}}_T) := \int_T G_T^k(\underline{\mathbf{w}}_T; \underline{\mathbf{v}}_T) \cdot \mathbf{z}_T + \frac{1}{2} \int_T D_T^{2k} \underline{\mathbf{w}}_T(\mathbf{v}_T \cdot \mathbf{z}_T) \\ + \frac{1}{2} \sum_{F \in \mathcal{F}_T} \int_F (\mathbf{w}_F \cdot \mathbf{n}_{TF})(\mathbf{v}_F - \mathbf{v}_T) \cdot (\mathbf{z}_F - \mathbf{z}_T)$$

- The second and third terms embody **Temam's device**

Discrete problem I

- The discrete problem reads: Find $(\underline{\mathbf{u}}_h, p_h) \in \underline{\mathbf{U}}_{h,0}^k \times P_h^k$ s.t.

$$\begin{aligned} \nu a_h(\underline{\mathbf{u}}_h, \underline{\mathbf{v}}_h) + t_h(\underline{\mathbf{u}}_h, \underline{\mathbf{u}}_h, \underline{\mathbf{v}}_h) + b_h(\underline{\mathbf{v}}_h, p_h) &= \int_{\Omega} \mathbf{f} \cdot \underline{\mathbf{v}}_h & \forall \underline{\mathbf{v}}_h \in \underline{\mathbf{U}}_{h,0}^k, \\ -b_h(\underline{\mathbf{u}}_h, q_h) &= 0 & \forall q_h \in P_h^k \end{aligned}$$

- Optionally, **upwind stabilisation** can be added through the term

$$j_h(\underline{\mathbf{w}}_h; \underline{\mathbf{v}}_h, \underline{\mathbf{z}}_h) := \sum_{T \in \mathcal{T}_h} \sum_{F \in \mathcal{F}_T} \int_F \frac{\nu}{h_F} \rho(\mathbf{P}_{e_{TF}}(\mathbf{w}_F)) (\mathbf{v}_F - \mathbf{v}_T) \cdot (\mathbf{z}_F - \mathbf{z}_T)$$

- **Weakly enforced boundary conditions** can also be considered

Theorem (Existence and a priori bounds)

There exists a solution $(\underline{\mathbf{u}}_h, p_h) \in \underline{U}_{h,0}^k \times P_h^k$ such that

$$\|\underline{\mathbf{u}}_h\|_{1,h} \lesssim \nu^{-1} \|\mathbf{f}\|_{L^2(\Omega)^d}, \text{ and } \|p_h\| \lesssim \left(\|\mathbf{f}\|_{L^2(\Omega)^d} + \nu^{-2} \|\mathbf{f}\|_{L^2(\Omega)^d}^2 \right),$$

with hidden constant independent of h and ν .

Theorem (Uniqueness of the discrete solution)

Assume that the forcing term verifies

$$\|\mathbf{f}\|_{L^2(\Omega)^d} \leq C\nu^2$$

with C hidden constant independent of h and ν small enough. Then, the solution is unique.

Theorem (Convergence to minimal regularity solutions)

It holds up to a subsequence, as $h \rightarrow 0$,

- $\mathbf{u}_h \rightarrow \mathbf{u}$ strongly in $L^p(\Omega)^d$ for $\begin{cases} p \in [1, +\infty) & \text{if } d = 2, \\ p \in [1, 6) & \text{if } d = 3; \end{cases}$
- $\mathbf{G}_h^k \underline{\mathbf{u}}_h \rightarrow \nabla \mathbf{u}$ strongly in $L^2(\Omega)^{d \times d}$;
- $s_h(\underline{\mathbf{u}}_h, \underline{\mathbf{u}}_h) \rightarrow 0$;
- $p_h \rightarrow p$ strongly in $L^2(\Omega)$.

If the exact solution is unique, then the whole sequence converges.

Key tools: discrete **Sobolev embeddings** and **Rellick–Kondrachov compactness results** from [DP and Droniou, 2017a]

Convergence II

Theorem (Convergence rates for small data)

Assume uniqueness for both $(\underline{\mathbf{u}}_h, p_h)$ and (\mathbf{u}, p) . Assume, moreover, the additional regularity $(\mathbf{u}, p) \in H^{k+2}(\Omega)^d \times H^{k+1}(\Omega)$, as well as

$$\|\mathbf{f}\|_{L^2(\Omega)^d} \leq C\nu^2$$

with C independent of h and ν small enough. Then, with hidden constant independent of h and ν ,

$$\|\underline{\mathbf{u}}_h - \underline{\mathbf{I}}_h^k \mathbf{u}\|_{1,h} + \nu^{-1} \|p_h - \pi_h^{0,k} p\|_{L^2(\Omega)} \lesssim h^{k+1} \mathcal{N}_{\mathbf{u},p}.$$

with $\mathcal{N}_{\mathbf{u},p} := (1 + \nu^{-1} \|\mathbf{u}\|_{H^2(\Omega)^d}) \|\mathbf{u}\|_{H^{k+2}(\Omega)^d} + \nu^{-1} \|p\|_{H^{k+1}(\Omega)}$.

Static condensation

- Partition the discrete velocity unknowns as before, and the pressure unknowns into **average value + oscillations** inside each element
- At each iteration, the linear system has the form

$$\begin{bmatrix} \mathbf{A}_{\mathcal{T}_h \mathcal{T}_h} & \tilde{\mathbf{B}}_{\mathcal{T}_h} & \mathbf{A}_{\mathcal{T}_h \mathcal{F}_h^i} & \bar{\mathbf{B}}_{\mathcal{T}_h} \\ \mathbf{A}_{\mathcal{F}_h^i \mathcal{T}_h} & \tilde{\mathbf{B}}_{\mathcal{F}_h^i} & \mathbf{A}_{\mathcal{F}_h^i \mathcal{F}_h^i} & \bar{\mathbf{B}}_{\mathcal{F}_h^i} \\ \tilde{\mathbf{B}}_{\mathcal{T}_h}^T & 0 & \tilde{\mathbf{B}}_{\mathcal{F}_h^i}^T & 0 \\ \bar{\mathbf{B}}_{\mathcal{T}_h}^T & 0 & \bar{\mathbf{B}}_{\mathcal{F}_h^i}^T & 0 \end{bmatrix} \begin{bmatrix} \mathbf{U}_{\mathcal{T}_h} \\ \tilde{\mathbf{P}}_{\mathcal{T}_h} \\ \mathbf{U}_{\mathcal{F}_h^i} \\ \bar{\mathbf{P}}_{\mathcal{T}_h} \end{bmatrix} = \begin{bmatrix} \mathbf{F}_{\mathcal{T}_h} \\ 0 \\ 0 \\ 0 \end{bmatrix}$$

- Static condensation of $\mathbf{U}_{\mathcal{T}_h}$ and $\tilde{\mathbf{P}}_{\mathcal{T}_h}$ is possible

Convergence rate: Kovasznay flow

- Following [Kovasznay, 1948], let $\Omega := (-0.5, 1.5) \times (0, 2)$ and set

$$\text{Re} := (2\nu)^{-1}, \quad \lambda := \text{Re} - (\text{Re}^2 + 4\pi^2)^{\frac{1}{2}}$$

- The components of the velocity are given by

$$u_1(\mathbf{x}) := 1 - \exp(\lambda x_1) \cos(2\pi x_2), \quad u_2(\mathbf{x}) := \frac{\lambda}{2\pi} \exp(\lambda x_1) \sin(2\pi x_2),$$

and pressure given by

$$p(\mathbf{x}) := -\frac{1}{2} \exp(2\lambda x_1) + \frac{\lambda}{2} (\exp(4\lambda) - 1)$$

- We monitor the errors

$$\mathbf{e}_h := \underline{\mathbf{u}}_h - \underline{\mathbf{I}}_h^k \mathbf{u}, \quad \epsilon_h := p_h - \pi_h^{0,k} p$$

Convergence rate: Kovasznay flow

Strongly enforced BC, upwind stabilisation, $Re = 40$

N_{dof}	N_{nz}	$\ e_h\ _{V,h}$	EOC	$\ e_h\ _{L^2(\Omega)d}$	EOC	$\ \epsilon_h\ _{L^2(\Omega)}$	EOC	τ_{ass}	τ_{sol}
$k = 0$									
65	736	9.37e-01	-	1.40e-01	-	6.84e-01	-	1.31e-02	8.52e-03
289	3808	1.13e+00	-0.27	5.50e-01	-1.98	1.96e-01	1.80	5.92e-02	4.90e-02
1217	17056	9.14e-01	0.31	2.26e-01	1.28	1.02e-01	0.94	1.02e-01	1.06e-01
4993	71968	6.26e-01	0.55	7.89e-02	1.52	3.52e-02	1.54	3.10e-01	4.46e-01
20225	295456	3.87e-01	0.70	2.47e-02	1.68	9.78e-03	1.85	1.02e+00	2.17e+00
81409	1197088	2.47e-01	0.65	8.06e-03	1.61	3.09e-03	1.66	3.73e+00	1.49e+01
$k = 1$									
113	2464	7.31e-01	-	5.37e-01	-	2.49e-01	-	2.51e-02	1.72e-02
513	13056	3.83e-01	0.93	1.54e-01	1.80	4.29e-02	2.54	4.77e-02	4.72e-02
2177	59008	1.02e-01	1.90	2.13e-02	2.85	3.98e-03	3.43	1.29e-01	1.79e-01
8961	249984	2.93e-02	1.80	2.97e-03	2.84	6.54e-04	2.61	5.13e-01	1.01e+00
36353	1028224	8.23e-03	1.83	3.99e-04	2.90	1.28e-04	2.35	2.05e+00	5.28e+00
146433	4169856	2.26e-03	1.86	5.21e-05	2.94	2.65e-05	2.27	7.25e+00	2.97e+01
$k = 2$									
161	5216	3.50e-01	-	2.09e-01	-	6.42e-02	-	3.44e-02	2.26e-02
737	27872	3.76e-02	3.22	1.34e-02	3.96	2.07e-03	4.95	6.95e-02	6.88e-02
3137	126368	6.96e-03	2.43	1.31e-03	3.36	1.48e-04	3.80	2.66e-01	3.60e-01
12929	536096	1.06e-03	2.72	9.48e-05	3.79	1.77e-05	3.07	1.11e+00	2.02e+00
52481	2206496	1.55e-04	2.77	6.36e-06	3.90	2.27e-06	2.96	4.16e+00	1.13e+01
211457	8951072	2.21e-05	2.81	4.13e-07	3.95	2.72e-07	3.06	1.51e+01	6.02e+01
$k = 5$									
305	19616	2.28e-03	-	1.05e-03	-	1.70e-04	-	1.28e-01	5.63e-02
1409	105728	4.01e-05	5.83	1.05e-05	6.65	2.05e-06	6.37	3.95e-01	2.19e-01
6017	480896	7.21e-07	5.80	8.98e-08	6.87	3.21e-08	6.00	1.60e+00	1.32e+00
24833	2043008	1.37e-08	5.72	7.89e-10	6.83	5.43e-10	5.88	6.45e+00	8.29e+00
100865	8414336	2.56e-10	5.74	6.72e-12	6.88	9.14e-12	5.89	2.54e+01	5.01e+01

Convergence rate: Kovasznay flow

Weakly enforced BC, no stabilisation, $Re = 40$

N_{dof}	N_{nz}	$\ e_h\ _{V,h}$	EOC	$\ e_h\ _{L^2(\Omega)d}$	EOC	$\ \epsilon_h\ _{L^2(\Omega)}$	EOC	τ_{ass}	τ_{sol}
$k = 0$									
97	1216	1.07e+00	–	3.93e-01	–	6.80e-01	–	2.68e-02	2.31e-02
353	4800	1.70e+00	-0.67	9.58e-01	-1.28	2.79e-01	1.28	3.41e-02	3.71e-02
1345	19072	1.44e+00	0.24	3.89e-01	1.30	1.32e-01	1.09	6.68e-02	8.04e-02
5249	76032	8.77e-01	0.72	1.18e-01	1.72	4.93e-02	1.42	2.15e-01	3.52e-01
20737	303616	4.78e-01	0.88	3.23e-02	1.87	1.49e-02	1.72	8.07e-01	1.95e+00
82433	1213440	2.46e-01	0.96	8.32e-03	1.96	4.08e-03	1.87	3.19e+00	1.47e+01
$k = 1$									
177	4256	1.02e+00	–	7.27e-01	–	2.69e-01	–	1.44e-02	1.60e-02
641	16768	4.20e-01	1.28	1.66e-01	2.13	4.96e-02	2.44	3.59e-02	4.25e-02
2433	66560	1.40e-01	1.58	2.66e-02	2.64	8.60e-03	2.53	1.09e-01	1.70e-01
9473	265216	4.06e-02	1.79	3.55e-03	2.91	1.29e-03	2.74	4.62e-01	1.10e+00
37377	1058816	1.03e-02	1.97	4.37e-04	3.02	1.79e-04	2.85	1.91e+00	5.64e+00
148481	4231168	2.61e-03	1.99	5.46e-05	3.00	2.96e-05	2.60	7.07e+00	3.32e+01
$k = 2$									
257	9152	5.50e-01	–	3.16e-01	–	1.20e-01	–	2.23e-02	2.33e-02
929	36032	7.58e-02	2.86	2.46e-02	3.68	6.03e-03	4.31	6.11e-02	7.47e-02
3521	142976	1.23e-02	2.62	1.84e-03	3.74	3.69e-04	4.03	2.41e-01	3.90e-01
13697	569600	1.70e-03	2.86	1.12e-04	4.03	3.63e-05	3.35	1.02e+00	2.21e+00
54017	2273792	2.21e-04	2.95	6.87e-06	4.03	3.84e-06	3.24	3.62e+00	1.17e+01
214529	9085952	2.80e-05	2.98	4.28e-07	4.00	3.72e-07	3.37	1.40e+01	6.76e+01
$k = 5$									
497	34976	6.48e-03	–	1.76e-03	–	1.02e-03	–	1.23e-01	7.22e-02
1793	137600	7.07e-05	6.52	1.34e-05	7.04	4.58e-06	7.81	4.06e-01	2.95e-01
6785	545792	1.28e-06	5.79	1.10e-07	6.94	4.40e-08	6.70	1.51e+00	1.56e+00
26369	2173952	2.20e-08	5.87	8.84e-10	6.95	5.86e-10	6.23	5.67e+00	8.48e+00
103937	8677376	3.56e-10	5.95	7.20e-12	6.94	7.42e-12	6.30	2.28e+01	5.14e+01

Lid-driven cavity I

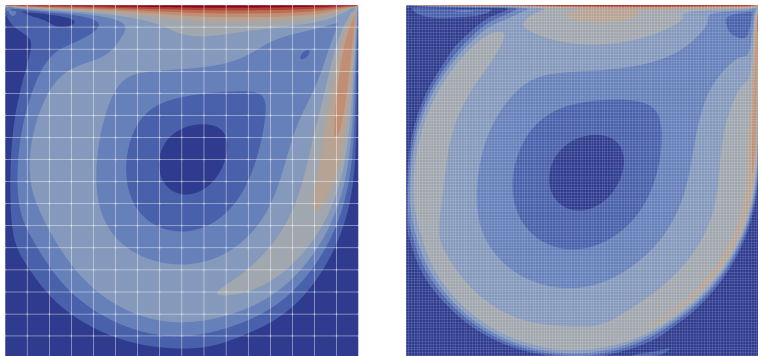


Figure: Lid-driven cavity, velocity magnitude contours (10 equispaced values in the range $[0, 1]$) for $k = 7$ computations at $Re = 1,000$ (left: 16×16 grid) and $Re = 20,000$ (right: 128×128 grid).

Lid-driven cavity

Re = 1,000

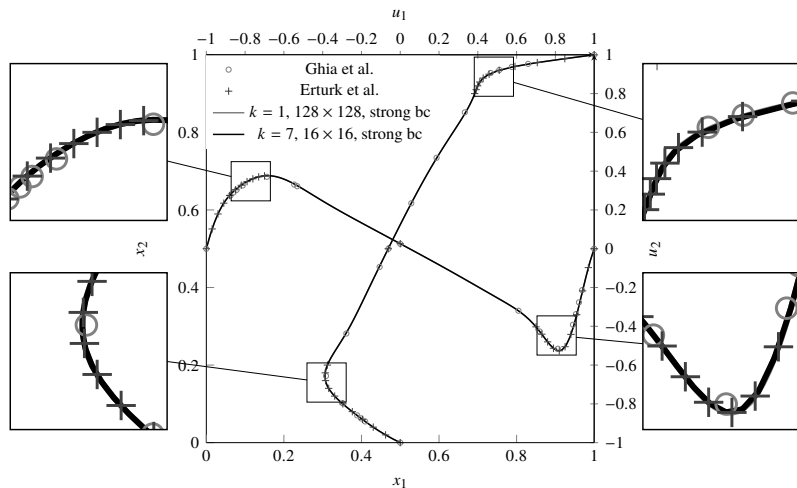


Figure: u_1 along the vertical centerline, u_2 along the horizontal centerline

Lid-driven cavity

Re = 5,000

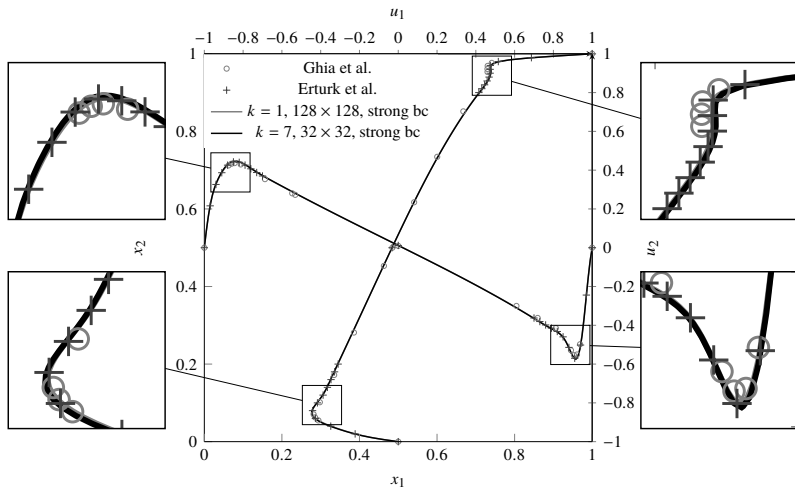


Figure: u_1 along the vertical centerline, u_2 along the horizontal centerline

Lid-driven cavity

Re = 10,000

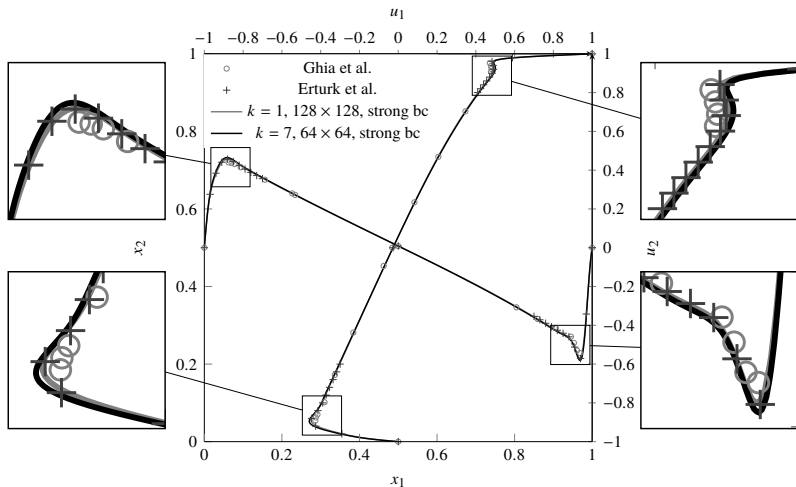


Figure: u_1 along the vertical centerline, u_2 along the horizontal centerline

Lid-driven cavity

Re = 20,000

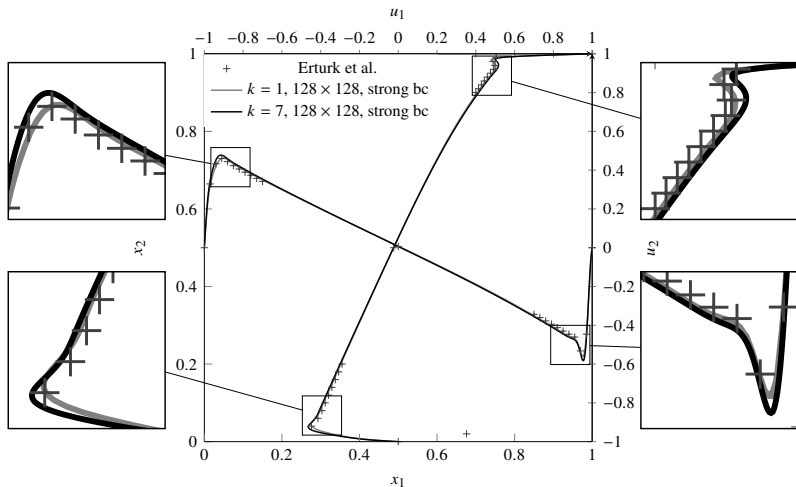


Figure: u_1 along the vertical centerline, u_2 along the horizontal centerline

Three-dimensional lid-driven cavity

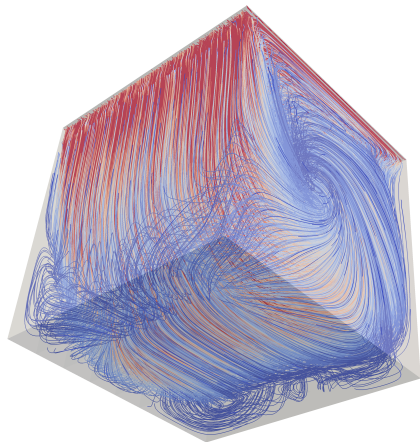


Figure: Three-dimensional lid-driven cavity, $Re = 1000$, streamlines

Lid-driven cavity

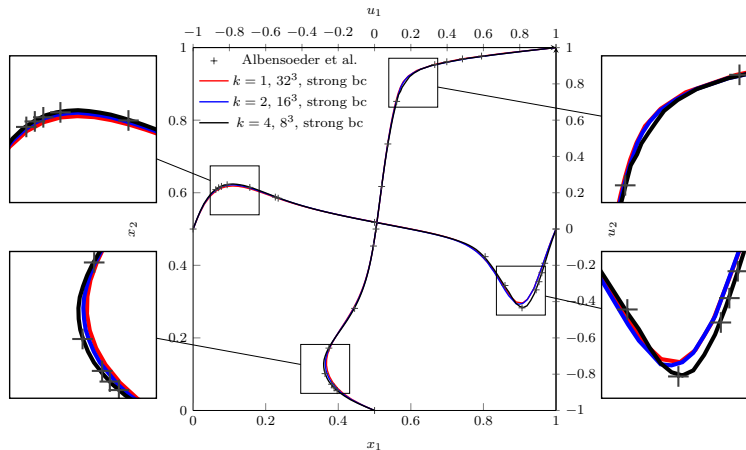


Figure: 3D Lid-driven cavity flow, horizontal component u_1 of the velocity along the vertical centerline $x_1, x_3 = \frac{1}{2}$ and the vertical component u_2 of the velocity along the horizontal centerline $x_2, x_3 = \frac{1}{2}$ for $Re = 1,000$, $k = 1, 2, 4$

Lid-driven cavity

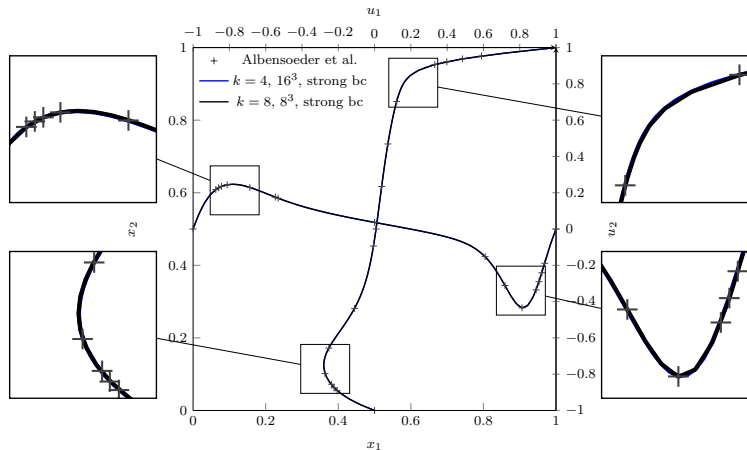


Figure: 3D Lid-driven cavity flow, horizontal component u_1 of the velocity along the vertical centerline $x_1, x_3 = \frac{1}{2}$ and the vertical component u_2 of the velocity along the horizontal centerline $x_2, x_3 = \frac{1}{2}$ for $\text{Re} = 1,000$, $k = 4, 8$

References I



Aghili, J., Boyaval, S., and Di Pietro, D. A. (2015).

Hybridization of mixed high-order methods on general meshes and application to the Stokes equations.
Comput. Meth. Appl. Math., 15(2):111–134.



Aghili, J. and Di Pietro, D. A. (2018).

An advection-robust Hybrid High-Order method for the Oseen problem.
J. Sci. Comput.
Published online.



Botti, L., Di Pietro, D. A., and Droniou, J. (2018).

A Hybrid High-Order discretisation of the Brinkman problem robust in the Darcy and Stokes limits.
Comput. Meth. Appl. Mech. Engrg., 341:278–310.



Botti, L., Di Pietro, D. A., and Droniou, J. (2019).

A Hybrid High-Order method for the incompressible Navier–Stokes equations based on Temam’s device.
J. Comput. Phys., 376:786–816.



Di Pietro, D. A. and Droniou, J. (2017a).

A Hybrid High-Order method for Leray–Lions elliptic equations on general meshes.
Math. Comp., 86(307):2159–2191.



Di Pietro, D. A. and Droniou, J. (2017b).

$W^{S,P}$ -approximation properties of elliptic projectors on polynomial spaces, with application to the error analysis of a Hybrid High-Order discretisation of Leray–Lions problems.
Math. Models Methods Appl. Sci., 27(5):879–908.



Di Pietro, D. A. and Droniou, J. (2018).

A third Strang lemma for schemes in fully discrete formulation.
Calcolo, 55(40).

References II



Di Pietro, D. A. and Ern, A. (2015).

A hybrid high-order locking-free method for linear elasticity on general meshes.
Comput. Methods Appl. Mech. Engrg., 283:1–21.



Di Pietro, D. A., Ern, A., Linke, A., and Schieweck, F. (2016).

A discontinuous skeletal method for the viscosity-dependent Stokes problem.
Comput. Meth. Appl. Mech. Engrg., 306:175–195.



Di Pietro, D. A. and Krell, S. (2018).

A Hybrid High-Order method for the steady incompressible Navier–Stokes problem.
J. Sci. Comput., 74(3):1677–1705.



Di Pietro, D. A. and Specogna, R. (2016).

An a posteriori-driven adaptive Mixed High-Order method with application to electrostatics.
J. Comput. Phys., 326(1):35–55.



Di Pietro, D. A. and Tittarelli, R. (2018).

Numerical Methods for PDEs, chapter An introduction to Hybrid High-Order methods.
Number 15 in SEMA-SIMAI. Springer.



Kovaszny, L. S. G. (1948).

Laminar flow behind a two-dimensional grid.
Proc. Camb. Philos. Soc., 44:58–62.



Temam, R. (1979).

Navier-Stokes equations, volume 2 of *Studies in Mathematics and its Applications*.
North-Holland Publishing Co., Amsterdam-New York, revised edition.
Theory and numerical analysis, With an appendix by F. Thomasset.